RECENT PROGRESS IN X-RAY EMITTANCE DIAGNOSTICS AT SPRING-8

S. Takano*, M. Masaki
Japan Synchrotron Radiation Research Institute (JASRI/SPring-8), Hyogo 679-5198, Japan
H. Sumitomo
SPring-8 Service Co. Ltd. (SES), Hyogo 679-5165, Japan

Abstract

At the SPring-8 storage ring, we have recently developed two X-ray instruments for emittance diagnostics. The one for a bending magnet source is the X-ray pinhole camera which directly images the beam profile. A pinhole in the atmosphere is composed of combined narrow X-Y slits made of tungsten. A scintillator crystal is used to convert the X-ray beam image to a visible image. The spatial resolution is about 7 μm. It is operated for continuous emittance diagnostics and coupling correction of user operation of SPring-8. The other for an undulator source is the X-ray Fresnel diffractometry monitor. Monochromatic X-rays are cut out by a single slit, and the vertical beam size is deduced from the depth of the central dip in a double-lobed diffraction pattern. Resolving beam size less than 5 μm is feasible.

INTRODCUTION

Light source rings are competing to achieve lower emittance and emittance coupling ratio for higher brilliance. Serious and elaborate efforts are being paid for upgrade plans of existing synchrotron radiation (SR) rings or new plans of low emittance rings.

X-ray SR is the key diagnostics probe for non-destructive beam emittance [1]. Both direct imaging and interferometric techniques can resolve the micrometer-order transverse beam size. The beam emittance is obtained from the measured beam size with the knowledge of the betatron and dispersion functions and the beam energy spread.

At the SPring-8 storage ring, we have recently developed two X-ray instruments for emittance diagnostics. The one for a bending magnet source is the X-ray pinhole camera which directly images the beam profile. The spatial resolution is about 7 μm. It is operated for continuous emittance diagnostics and coupling correction of user operation of SPring-8. The other for an undulator source is the X-ray Fresnel diffractometry (XFD) monitor [2,3]. Monochromatic X-rays are cut out by a single slit, and the vertical beam size is deduced from the depth of the central dip in a double-lobed diffraction pattern. Resolving beam size less than 5 μm is feasible.

X-RAY PINHOLE CAMERA

The layout of the SPring-8 X-ray pinhole camera is shown in Fig. 1 and the specifications are summarized in Table 1.

The source point is in a dipole magnet (29B2), 1.0 mrad inside from the edge. The magnetic field and the critical photon energy of emitted X-rays is 0.5 T and 21.1 keV, respectively. The X-ray window is located at a distance of 6.2 m from the source point. The window material is aluminium alloy of 3 mm thickness. The window separates the ultra-high vacuum and the atmosphere, and the X-rays emitted in the source dipole magnet go out to the atmosphere.

The pinhole assembly in the atmosphere is located at a distance of 11.4 m from the source. It is composed of

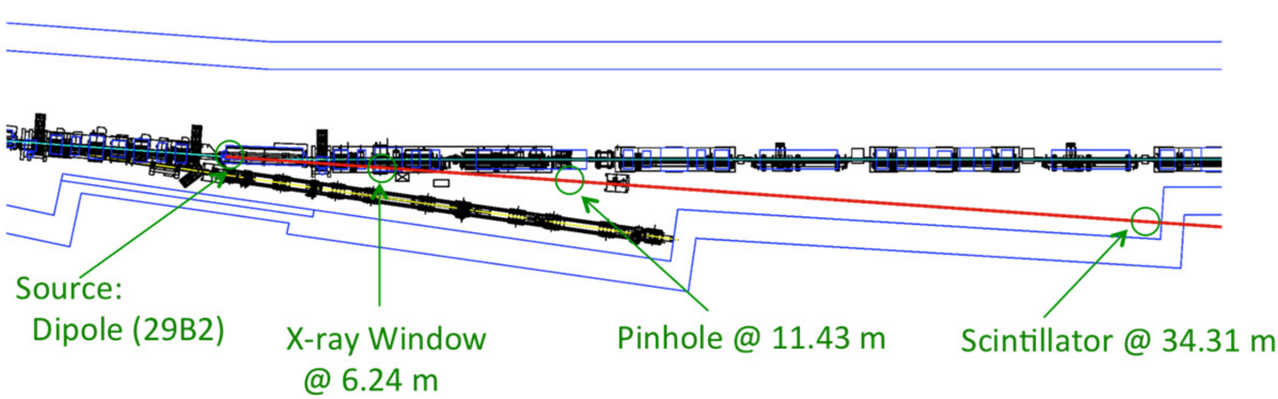

Figure 1: Layout of the X-ray pinhole camera of SPring-8.

*takano@spring8.or.jp

ISBN 978-3-95450-176-2

Table 1: Specifications of the SPring-8 X-ray Pinhole Camera

Light Source	Bending Magnent (29B2)	
Pinhole	Distance from Source (m)	11.4
	Aperture Size (μm)	20 x 20
Scintillator	Distance from Source (m)	34.3
	Material	$CdWO_4$
Camera	Number of Pixels	2448 x 2050
	Pixel Size (μm)	3.45 x 3.45
Magnification Factor	x 4 (Pinhole: x 2, Lens: x 2)	
Resolution (rms) (μm)	7.2 (Pinhole: 6.9, Scintillator & Camera: 2.2)	

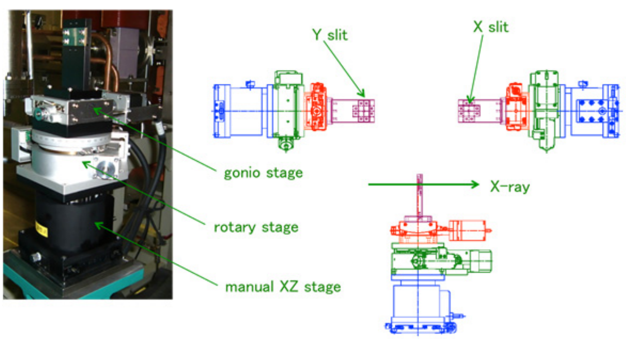

Figure 2: Pinhole assembly.

combined narrow X-Y slits made of tungsten (Fig. 2). The thickness of each slit is 3mm, and the aperture size of the pinhole is 20 μm x 20μm. The pinhole assembly is equipped with remote controllable gonio and rotary stages for adjustments of pitch and yaw of the pinhole. It is mounted on a manual XZ stage for alignment.

The X-ray image of the electron beam formed by the pinhole is converted to a visible image by a scintillator located at a distance 34.3 m from the source. The magnification factor of the pinhole is accordingly two. The visible image is measured by a CCD camera through a lens. The details of the scintillator and camera assembly

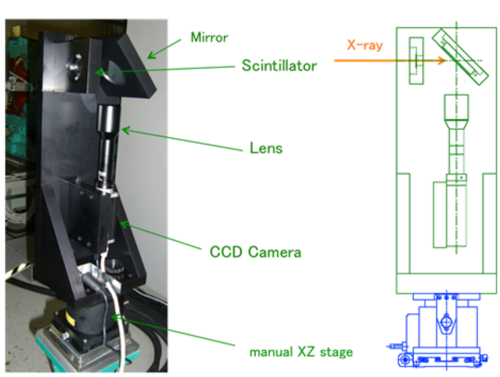

Figure 3: Scintillator and camera assembly

are shown in Fig. 3. The scintillator is made of CdW_4O with a thickness of 0.5mm. The lens is object-space telecentric with a magnification factor of two. The CCD camera (Basler AG, piA2400-17gm) has 2448 x 2050 square pixels of 3.45 μm size. It is connected to a remote computer through the Gig-E (Gigabit Ethernet) interface.

The total spatial resolution of the pinhole camera σ_{XPC} is expressed as,

$$\sigma_{XPC} = \sqrt{\sigma_{diff}^2 + \sigma_{CAM}^2} \quad (1)$$

where σ_{diff} stands for the contribution of diffraction of pinhole and σ_{CAM} for that of the scintillator and camera assembly.

The pinhole resolution σ_{diff} was evaluated according to numerical calculation of the point-spread function (PSF) based on wave optics by using diffraction formula. Examples of PSFs of the pinhole for monochromatic X-rays, pinhole diffraction patterns for a monochromatic point source, are shown in Figs. 4(a) and (b). The resolution σ_{diff} was defined by width of a Gaussian curve fitted to the PSF. Fig. 5 (a) shows the monochromatic pinhole resolution as a function of the X-ray energy.

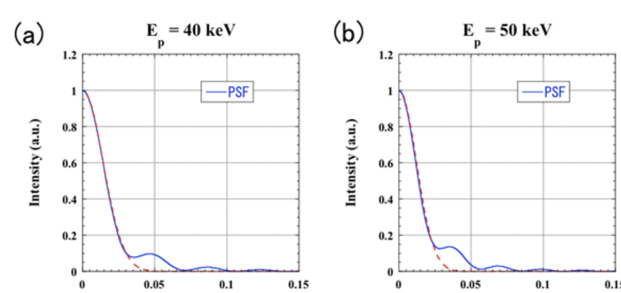

Figure 4: Examples of the point-spread functions (PSFs) of the pinhole for monochromatic X-rays (blue), and fitted Gaussian curves (red).

ISBN 978-3-95450-176-2

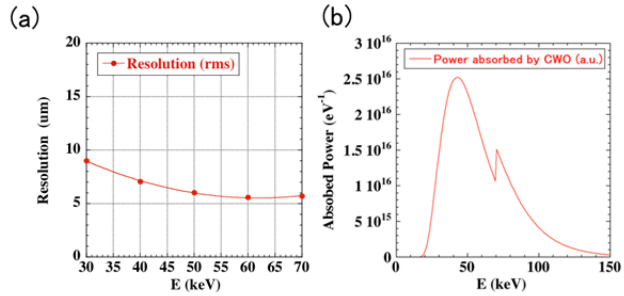

Figure 5: (a) Monochromatic pinhole resolution as a function of the X-ray energy. (b) Spectral power absorbed by the scintillator.

Spectral power absorbed by the scintillator was calculated by the calculation code SPECTRA [4], and found to peak at an X-ray energy of 42 keV as shown in Fig. 5(b). The resolution of the pinhole σ_{diff} was evaluated to be 6.9 µm from the width of the monochromatic PSF at 42 keV.

The resolution of the scintillator and camera assembly σ_{CAM} was calibrated by the sharpness of the observed edge of a tungsten bar placed in front of the scintillator. Fig. 6(a) shows the tungsten bar and 6(b) an observed

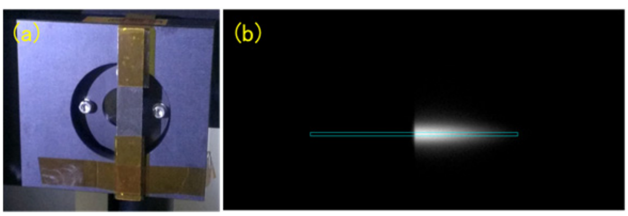

Figure 6: (a) Tungsten bar placed in front of the scintillator for calibration of the resolution of the scintillator and camera assembly. (b) Edge of the bar observed in a beam image.

beam image with an edge cut by the bar. The profile of the observed edge and its derivative are shown in Figs. 7(a) and (b). The resolution σ_{CAM} of the scintillator and

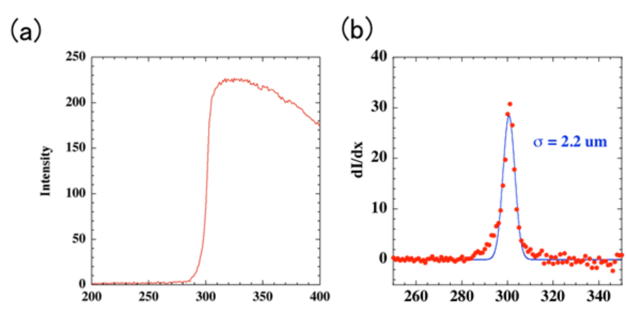

Figure 7: (a) Profile of the observed edge with the bar. (b) The derivative of the edge profile (red) and a fitted Gausiian curve (blue).

camera assembly was evaluated as 2.2 µm on the beam coordinate (4.4 µm on the scintillator) from the width of a Gaussian curve fitted to the derivative in Fig. 7(b). The total spatial resolution of the pinhole camera σ_{XPC} given by Eq. (1) is accordingly 7.2 µm.

The scale of the camera pixel to the beam coordinate was calibrated by introducing vertical bump orbits (Fig. 8). The calibrated scale is 0.848 µm/pixel, which is

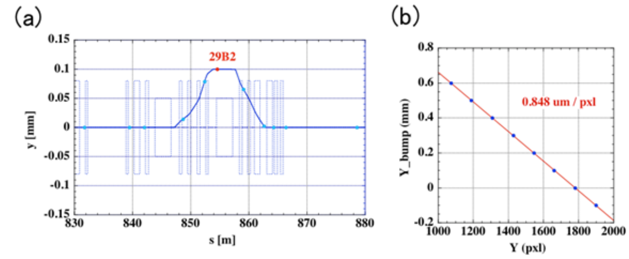

Figure 8: (a) Schematic of the vertical bump orbit. (b) The observed relation between the beam position and the image position on the CCD camera.

consistent with the designed value of 0.863 µm/pixel within the manufacturer's specified accuracy of the lens magnification factor.

The display for the X-ray pinhole camera in the SPring-8 control room is sown in Fig. 9. Live beam image view

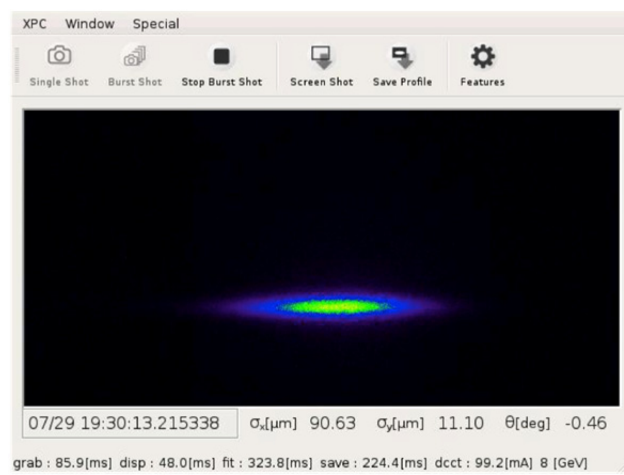

Figure 9: The display for the X-ray pinhole camera in the SPring-8 control room.

is available with the refreshing rate of approximately 15 frames per seconds.

Parameters of the beam profile, including the horizontal and vertical bean sizes σ_x and σ_y and the beam tilt angle θ, are obtained periodically with a cycle time of 1s by fitting a two-dimensional Gaussian profile to the beam image. They are logged to the control system database.

The SPring-8 X-ray pinhole camera was installed in March 2014. After commissioning and calibration, it has been operating as a real time emittance diagnostics since September 2014. It is a indispensable diagnostics tool for both beam tuning and user operation of SPring-8.

ISBN 978-3-95450-176-2

X-RAY FRESNEL DIFFRACTOMETRY MONITOR (XFD)

X-ray Fresnel diffractometry monitor (XFD) is a diagnostic technique for light source rings to measure vertical beam size at ID (undulator) source point [2,3]. Schematics of XFD are illustrated in Fig. 10. It employs a

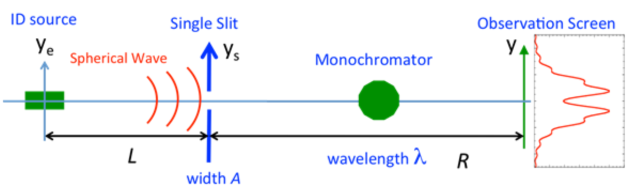

Figure 10: Schematics of X-ray Fresnel diffractometry monitor (XFD).

single slit and a monochrometer and an imaging device (X-ray camera). Diffraction patterns observed on the screen of the imaging device depend on a width A of the slit. By adequitely tuning the slit width, a double-lobed Fresnal diffraction pattern is available. The optimum slit width for the deepest median dip is expressed as,

$$A \approx \sqrt{7\lambda \frac{LR}{L+R}}.$$

The depth of the median dip correlates with the light source size.

The setup for the initial XFD experiment at SPring-8 is shown in Fig. 11 [2,3]. The source is a planar undulator

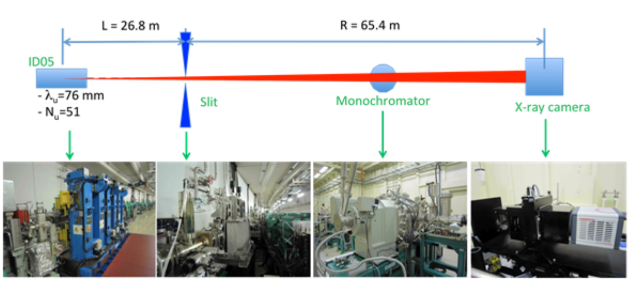

Figure 11: Setup for the initial XFD experiment at SPring-8.

(ID05) with 51 magnetic periods of 76 mm long. The vertical beam size at the source point of ID05 smaller than 10 μm was successfully resolved [2,3].

In order to improve the performance of the XFD, we have recently replaced an X-ray imaging device and increased the observing photon energy. The new setup

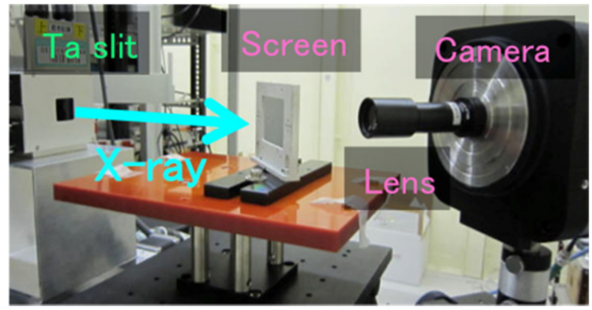

Figure 12: New X-ray imaging setup for XFD experiment at SPring-8.

for X-ray imaging is shown in Fig. 12. The screen material is YAG(Ce) of 50 μm thick. The pixel size of the camera is 16 μm x 16 μm. Minimum available exposure time of the camera is 0.2 ms five times shorter than that of the previous camera of 1ms. The shorter exposure time reduces the influence of the vibration of the cryogenically cooled monochromator crystals. The resolution of the X-ray imaging device was calibrated by the sharpness of the observed edge of a tantalum slit installed in front of the screen. The obtained resolution as converted to the source

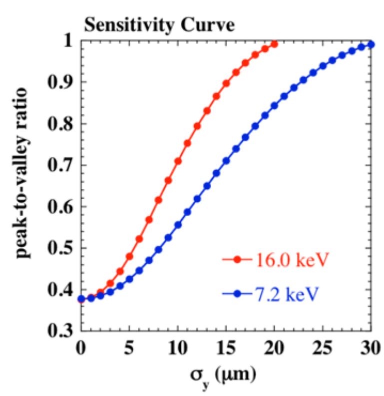

Figure 13: Sensitivity curve of XFD for the increased observing energy 16 keV (red) and for the previous 7.2 keV (blue).

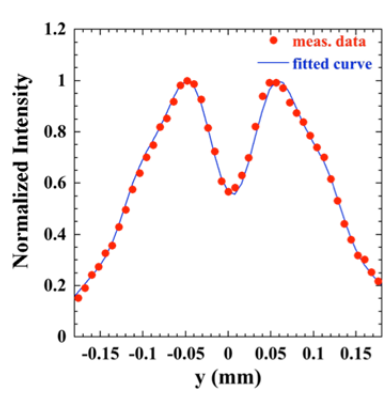

Figure 14: Example of observed diffraction pattern (red) and fitted model function (blue). The deduced source vertical beam size is 6.3 μm (rms).

ISBN 978-3-95450-176-2

point coordinate is 2.2 µm, which is three times better than the previous device. The sensitivity curve, peak-to-valley-ratio of the median dip of the double-lobed diffraction pattern as a function of vertical beam size, is shown in Fig. 13. Improvement of the sensitivity for small beam size below 5 µm is evident for the increased observing energy (16 keV). An example of diffraction pattern observed with the new imaging device at the increased X-ray energy (16keV) is shown in Fig. 14. By fitting the theoretical model function [3] to data, vertical beam size (rms) of 6.3 µm was deduced.

CONCLUSION

The SPring-8 X-ray pinhole camera was installed in March 2014. It images a dipole magnet source with a spatial resolution (rms) of 7.2 µm. It has been operating since September 2014 as a real time emittance diagnostics indispensable for both beam tuning and user operation of SPring-8.

The XFD developed at SPring-8 is a diagnostic technique for light source rings to measure vertical beam size at ID (undulator) source point, feasible to resolve beam size smaller than 5 µm (rms). It requires only slit, monochromator, and imaging device (X-ray camera), and has potential universal availability to ID beamlines of the diffraction limited storage rings (DLSRs).

REFERENCES

[1] S. Takano, “Beam Diagnostics with Synchrotron Radiation in Light Sourecs”, IPAC’10, p2392. (2010).

[2] M. Masaki, Y. Shimosaki, S. Takano, M. Takao, “Novel Emittance Diagnostics for Diffraction Limited Light Sources Based on X-ray Fresnel Diffractometry”, IBIC’14, p274. (2014).

[3] M. Masaki, S. Takano, M. Takao Y. Shimosaki, “X-ray Fresnel diffractometry for ultralow emittance diagnostics of next generation synchrotron light sources.”, Phys. Rev. ST Accel. Beams 18, 042802 (2015).

[4] T. Tanaka and H. Kitamura, “SPECTRA: a Synchrotron Radiation Calculation Code”, J. Synchrotron Radiat. 8, 1221 (2001). http://radiant.harima.riken.go.jp/spectra/index.html

ISBN 978-3-95450-176-2